

Porous silicon based Bragg reflectors and Fabry-Perot interference filters for photonic applications

Dharmalingam Mangaiyarkarasi^a, Mark B H Breese^a, Ow Yueh Sheng^a, Kambiz Ansari^a
Chellappan Vijila^b, and Daniel Blackwood^c

^aCentre for Ion Beam Applications, 2 Science Drive 3, Department of Physics,
National University of Singapore, Singapore 117542

^bInstitute of Materials Research Engineering, 3 Research Link Singapore 117602

^cDepartment of Materials Science, National University of Singapore, Singapore 117542

ABSTRACT

Visible light emission from the porous silicon (PSi) formed by anodic etching of Si in HF solution has raised great interest in view of possible applications of Si based devices in optoelectronics. In particular, multilayers consisting of periodic repetition of two PSi layers whose refractive indices are different can be exploited to design interference filters for controlling the emission wavelength as well as for the spectral narrowing of the wide emission band of Psi. Fabry-Perot optical microcavities with an active layer of $\lambda/2$ or λ sandwiched between two Bragg reflectors, consisting of alternating layers of high and low refractive indices are fabricated on heavily doped p-type silicon. We have investigated the optical properties of these microstructures using reflectivity and photoluminescence measurements at various temperature.

Key words: Porous silicon, Bragg reflectors, Fabry-Perot filters, Photoluminescence, Reflection, microcavities

1.INTRODUCTION

Recent progress in semiconductor materials for optoelectronic applications have raised the hope of Silicon (Si) based optical interconnects for faster processes and high-speed communications. Although c-Si is the predominant material in semiconductor industry, the integration of optical communication and photonic technology with Si microelectronics had been inhibited by the fact that Si has an indirect band gap with poor optical emission efficiency.¹ A great deal of research effort has been focussed on nanometer size crystallites or quantum dots made from indirect-gap semiconductors.²⁻⁴ As a result, visible light emission from Si has been shown to be possible when it is in the form of a low-dimensional system or when selected active impurities (such as erbium) and/or new phases (such as iron disilicide) are inserted into the Si lattice.⁵ In particular, low-dimensional systems; such as silicon nanocrystals,⁶ porous silicon,^{2,3,7} silicon/insulator superlattices,⁸ silicon nanopillars⁹ are being actively investigated from viewpoints of both fundamental physics and optical devices.

1.1 Visible light emission from Porous silicon

Porous silicon, which forms on the surface of crystalline silicon in hydrofluoric acid under an appropriate anodic bias, has received intensive study over the last 15 years¹⁰⁻¹³ despite its discovery in 1956 by Uhlir.¹⁴ In 1990, Canham⁵ reported the efficient visible photoluminescence at room temperature, probably due to quantum confinement effects produced by the low dimensionality of the silicon skeleton remaining after electrochemical anodization.¹⁵ The typical luminescence spectrum is a broad band centered around 1.7 eV. The efficiency of this band is $\geq 1\%$ and its characteristic decay times are typically 1-10 μ sec at room temperature.¹⁶ Many efforts have been made to alter the peak wavelength emission from PSi, such as oxidation¹⁷ or photochemical etching^{18,19} or doping with rare earth compounds.²⁰ Also ambient PL over the full visible range from PSi was obtained through electrochemical etching aided by an oxidative metal such as Zn without post anodising treatment.^{21,22}

2. Optical microcavity

Despite the reasonable intensity of the PSi optical²³ and electro-optical emission,²⁴ practical device applications were not significant. This is mainly due to the very broad spectral and angular emissions and moreover ageing effects of the PSi.²⁵ The use of a microcavity structure, which is basically a combination of two dielectric mirrors is a well established tool to alter and control the spontaneous emission and has been realised in III-V semiconductor lasers.²⁶⁻²⁹

2.1 Distributed Bragg reflectors and Fabry–Perot interferometers

Dielectric mirrors, also called distributed Bragg reflectors (DBR) utilize the refractive index differences to achieve interferometric effects by forming periodic multilayer quarter wave stacks with alternating high and low refractive index layers. Various components of the incident light produced by reflection at successive boundaries through out the assembly will reappear at the front surface all in phase, so that they will recombine constructively. This implies that the effective reflectance of the assembly can be made very high indeed, as high as may be desired, merely by increasing the number of the layers. The reflectance remains high over only a limited range of wavelengths, depending on the ratio of high and low value of refractive index; outside this zone it changes abruptly to a low value. Due to this, the quarter wave stack is used as a building block for many types of thin film filters such as a long wave pass filter, as a short wave pass filter, as a straightforward high reflectance mirror and as a reflector in a thin film Fabry-Perot(F-P) interferometer.³⁰

Using two DBR separated by a spacer, which is a half wave thick; it is possible to construct a Fabry-Perot interference filter. Inserting a spacer into the dielectric structure breaks the periodicity of the dielectric and introduces a pass band into the transmission spectrum.³¹ Multiple beam interference in the spacer layer causes the transmission of the filter to be extremely high over a narrow band of wavelengths around that for which the spacer is a multiple of one half wavelength thick. Microcavities are formed by a layer structure similar to a F-P filter; a central active medium is embedded between two dielectric mirrors, which allow enhancement or inhibition of spontaneous emission at the energy of the cavity mode to be obtained, together with a highly directional emission.³²

2.2 Porous silicon based optical microcavity

Similarly, placing the silicon nanocrystals in a microcavity with dimensions comparable to optical wavelength reduces the spectral width of the PL spectrum of the active layer to the bandwidth of its resonant mode.³³⁻³⁵ This implies that if one couples the electron confinement with the photon confinement, the emission properties of silicon are further changed: a narrowing, an increase in the emission efficiency, and a strong directionality of the emission pattern are observed. By varying the applied current density, it is possible to change the porosity (percentage of void space) of the porous silicon film in the etching direction.¹⁸ Moreover the etching process is self-limited and the etching occurs only in pore tips. Thus the porosity varies only with current density once the other etching parameters are kept fixed,^{29,36} the formation of layers of alternating PSi layers of different porosity (and hence, different refractive index) results in dielectric multilayer structures that behave as optical interference filters, both in the infrared and VIS wavelength ranges.

Several groups have already demonstrated the fabrication of PS based Photonic band gap structures for many applications including DBRs and F-P filters,³⁷⁻³⁹ Rugate filters,⁴⁰ microcavities with controlled spontaneous emission,^{41,42} waveguides,^{43,44} and colour sensitive photodiodes.⁴⁵ Visible light emitting diodes based on PSi planar⁴⁶ and vertical⁴⁷ resonant cavities have been reported with tunable, narrow, and directional EL and PL spectral emissions.⁴⁸ Also random PSi multilayer structures⁴⁹ have been investigated theoretically and experimentally, since it is interesting in the field of one dimensional light localisation. Recently, Reece et al have reported the realization of optical microcavities with sub nanometer line widths at low temperature,⁵⁰ whereas multiple narrow transmission peaks in a limited region of the stop band are observed in free standing PS coupled optical microcavities by Ghulinyan et al.⁵¹

Previously, we reported that the PL emission characteristics of PSi can be precisely controlled by ion irradiation.⁵² We have demonstrated the use of focussed ion beam irradiation in conjunction with anodization to controllably alter the PL peak wavelength emission from adjacent micrometer sized areas of PSi.^{53,54} This resulted in PL images containing several distinct colour emissions, from green to red on 4 Ω -cm p-type silicon, whereas on heavily doped P-type silicon (0.02 Ω -cm), tuning of the PL intensity has been obtained by controlling the local resistivity with doses.⁵⁵ Though our interests is to extend ion irradiation studies on the multilayer structures, this paper mainly presents the preliminary work done so far on 0.02 Ω -cm silicon to characterise PSi multilayer parameters, such as refractive index and thickness measurement and also on the reflection and PL measurements from DBRs and F-P filter.

3.Results and discussion

3.1 Refractive index, thickness and porosity measurements

In order to form a microcavity with certain wavelength, appropriate index of refraction and thicknesses of alternating high and low index layers has to be chosen. The refractive index (n) of PS is lower than that of bulk Si, and decreases with increasing porosity, since it is basically a mixture of air and Si. The relationship between the porosity and n of each Psi layer is determined by various effective medium approximations.⁵⁶⁻⁵⁸ The n of PS is determined by its porosity, which depends on the current density (J) of the electro-chemical etching for a specific HF concentration and anodization time.^{59,60,37} The layer width (d) is determined by the etching time. Reference samples were prepared with different J at the same duration to measure n , d and porosity. In most articles on porous silicon, n has been determined from reflection measurements.³⁶ The energy between the peaks, associated with film thickness allows the determination of n . We have measured n of thick PS as a function of the wavelength, through reflectance measurements, by recording the spectral positions of the interference fringes³⁸ using equation (1),

$$n = \frac{1}{2d} \left(\frac{1}{\lambda_r} - \frac{1}{\lambda_{r+1}} \right)^{-1} \quad - \quad (1)$$

where d is the thickness & λ_r the wavelength of the r th fringe. The thickness and the etch rate of PSi samples were determined by SEM. Fig1a shows the spectral dependence of the n for the samples etched at different J . From these measurements a linear fit has been plotted for the refractive index profile of PSi films as well as their etch rate at different J , and are shown in Fig.1b and Fig.1c respectively. Maxwell–Garnet effective medium approximation⁵⁶ is used to calculate the porosity of the measured n samples at different J and has been plotted in Fig1d.

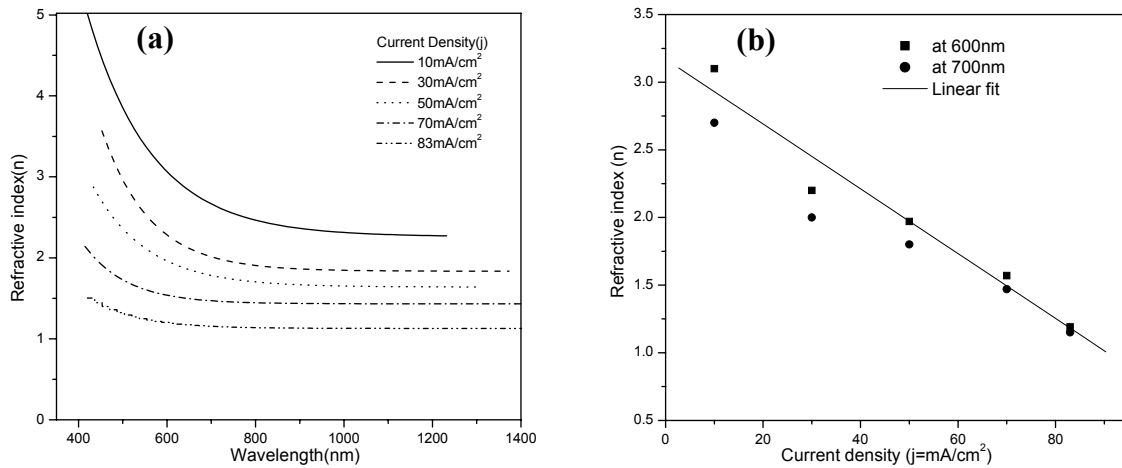


Fig1a. Measured indices of refraction for films prepared at different J Fig1b. Refractive index vs current density at two wavelengths

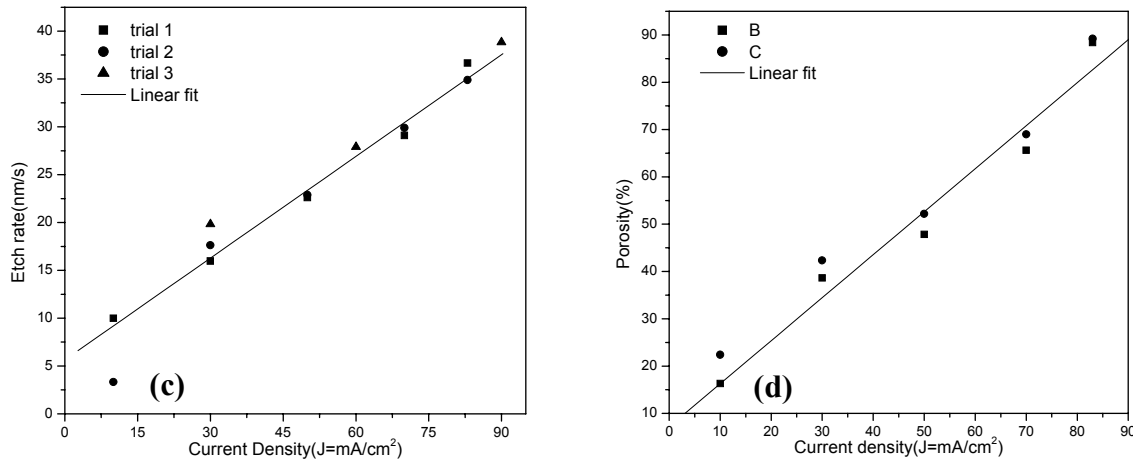


Fig.1c. Etch rate plot for PS films grown at different current densities

Fig.1d. Plot for porosity vs current density

3.2 Bragg Reflectors

DBRs are realised using a periodic modulation of the anodization currents. In order to obtain high reflectivity mirrors, 12 periods are used. Cross sectional SEM analysis of the DBR structures demonstrates the periodic variation of high and low porosity layers with smooth interfaces (Fig 2a). Fig2b shows the full colour reflectance emission from various DBRs. Fig2(c) & (d) shows the series of reflectivity spectra of DBRs at different wavelengths with (c) small and (d) large optical refractive index changes between the high and low porosity layers by changing the current density.

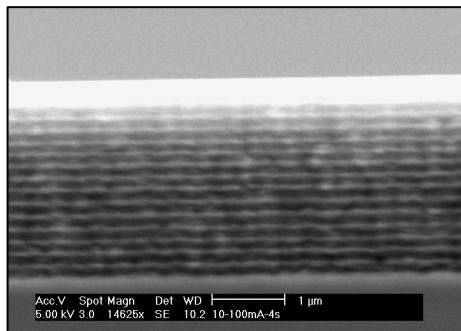


Fig 2a. Cross sectional SEM micrographs of DBRs consisting of 12 pairs of low (bright) and high (dark) porosity layers.

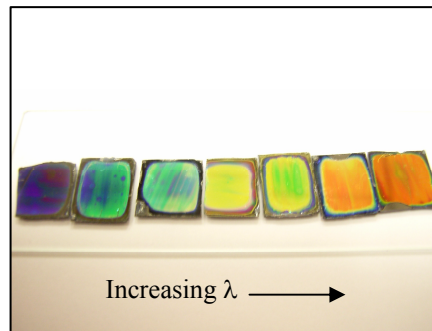


Fig 2b. Photograph of DBR samples prepared at different wavelength shows reflectance over the full visible range

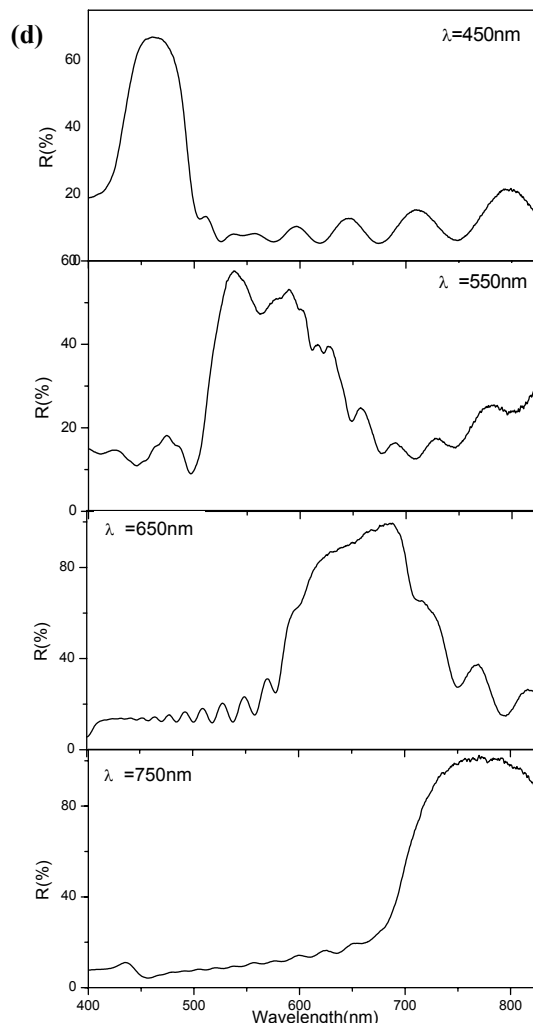
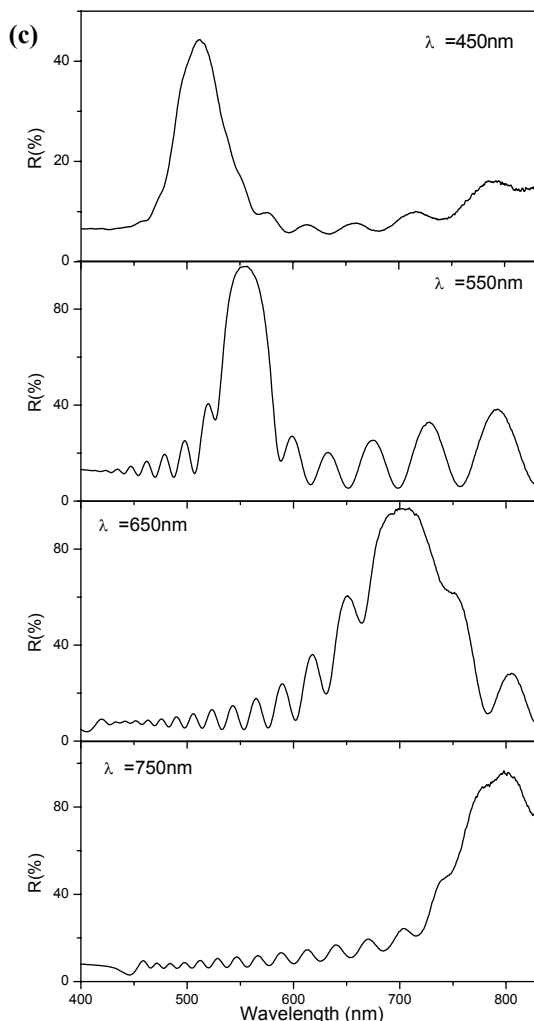


Fig 2c&d. Series of reflectivity spectra for complete visible range Bragg Reflectors consisting of high and low refractive index layers prepared with (c) $J=50$ & 85 mA/cm^2 and (d) 25 & 85 mA/cm^2

3.3 Fabry–Perot interferometers

For interference filters with narrow transmission characteristics a more complex layer structure is required. We have prepared F-P interferential filter by first forming the top DBR, then changing the anodization conditions to form the active layer, and finally forming the bottom DBR contain 12 pairs of low and high porosity layers all of which are $\lambda/4$ thick. Fig 3a shows a SEM micrograph of a F-P filter. The dark and light regions in SEM represent the high and low porosity layers of the Bragg reflectors, respectively. Though the contrast between the DBR layers are not very clear due to low magnification, the central active (multiple of $\lambda/2$ thick) layer, where λ is the wavelength of the cavity resonance can be clearly seen as a dark region (high porous). Moreover it is reported that using an optical interference filter on top of a highly luminescent PS layer the emission spectrum can be narrowed and the spectral peak maximum can be shifted. Therefore, a sample with a F-P filter on top of a 2 μ m thick luminescent layer has been formed and is shown in Fig 3b.

Reflectance spectra in Fig.3c shows the typical characteristics of an interferential FP filters where a transmittance maximum appears in the middle of the stop band at the wavelength of the F-P mode. In addition, by merely changing the F-P central wavelength, the peak transmittance wavelength can be tuned within the whole visible and IR ranges. All the F-P filter has the same structure formed by two equal DBR separated by a $\lambda/2$ thick central layer..

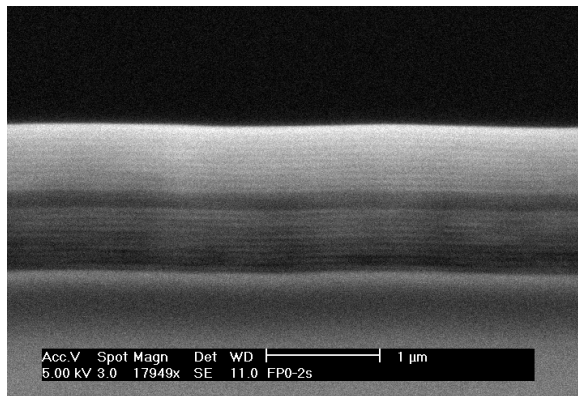


Fig3a. SEM micrograph Psi F-P filter without thick PSi

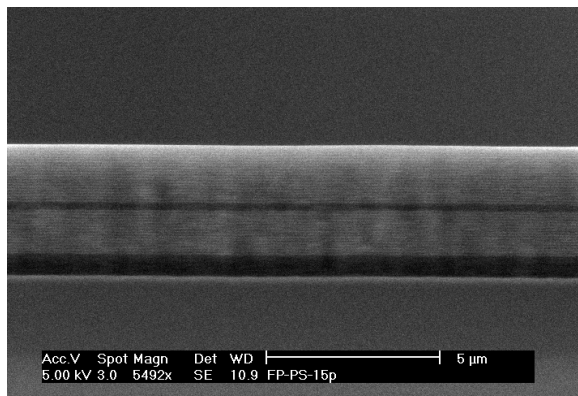


Fig. 3b. F-P filter formed at top of a 2m thick PS layer

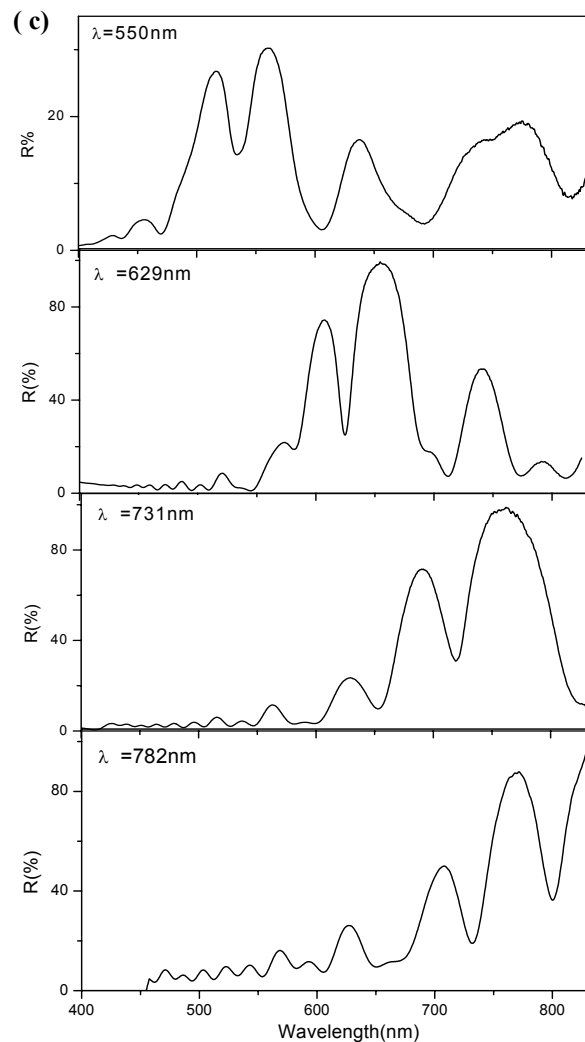


Fig 3c. Reflectance spectra of various wavelength F-P filters. Current densities used for the low and high porosity layers are 50 and 85mA/cm² and the same high current density (85mA/cm²) is applied to form central layer.

3.4 Photoluminescence from a F-P microcavity

PL measurements were performed using the 405nm line of He-Cd laser with a laser power of about 10mW. The PL light was detected along the z axis using a USB Ocean Optics spectrometer. Figure 4a & b shows the PL spectrum of the PSi microcavity structure taken at different temperatures. A low temperature photoluminescence measurement on the microcavity structure shows the enhancement effect at the resonant wavelength. The FWHM of the peak in the centre of the PL is 14nm. Compared to room temperature, a significant reduction has been achieved in the width of the emission band. However, tuning the filter above the PS band results in multiple peak emissions with broadband, which probably due to the strong light emission from the underlying PS layer in this range.

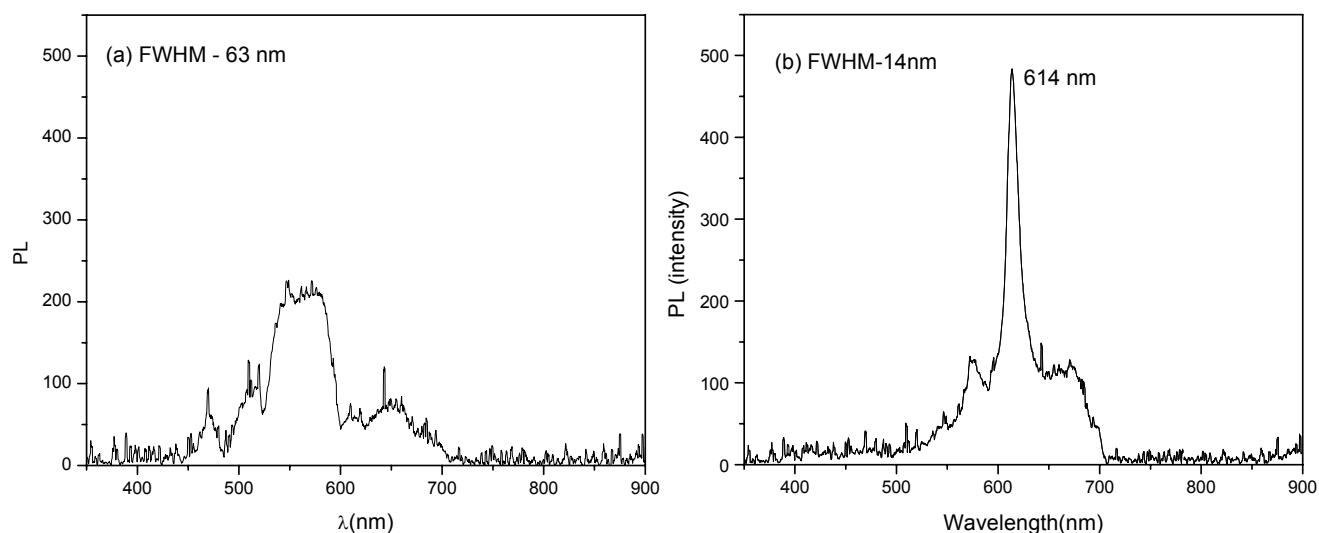


Fig 4. PL spectrum recorded on same PSi microcavity structure under (a) room and (b) liquid nitrogen temperatures

4. Conclusion

We have characterised the optical parameters for the porous silicon multilayer structures and fabricated a number of high quality Bragg reflectors and Fabry - Perot optical microcavities with tuning of emission wavelengths over wide range on heavily doped p-type silicon. We have investigated the optical properties of these microstructures using reflectivity and photoluminescence measurements at different temperatures. Furthermore, the effect of ion irradiation, which modifies the porous formation and hence the emission wavelength, is under investigation.

References

1. D.J.Lockwood, *Light emission in Silicon*, Academic press, Boston, 1997
2. L.T.Canham, *Appl.Phys.Lett.* 57, 1046, 1990.
3. A.G.Cullis and L.T.Canham, *Nature* 353, 335, 1991.
4. V.Lehman and U.Gosele, *Appl. Phys. Lett.* 58, 856, 1991
5. L.Pavesi, L.Dal Negro, C.Mazzoleni, G.Franzo and F.Prilo, *Nature* 408, 440, 2000.
6. W.L.Wilson, P.F.Szajowski and L.E.Brus, *Science* 262, 1242, 1993.

7. K.D.Hirschman, L.Tsybeskov, S.P.Duttagupta and P.M.Fauchet, *Nature* 384, 338, 1996.
8. Z.H.Lu, D.J.Lockhood and J.M.Baribeau, *Nature* 378, 258, 1995.
9. A.G.Nassiopulos, S.Grigoropoulos and D.Papadimitriou, *Appl. Phys.Lett.* 69, 2267, 1996.
10. M.I.J.Bcale, J.D.Benjamin, M.J.Uren, N.G.Chew and A.G.Cullis, *J.Cryst. Growth* 73, 622, 1985.
11. L.G.Earwaker, J.P.G.farr, P.E.Grzeszczyk, I.Sturland and J.M.Keen, *Nucl. Instrum. Methods Phys. Res. B* 9, 317, 1985
12. G.Bomchil, A.Halimaoui and R.Herino, *Microelectron. Eng.* 8, 293, 1988
13. R.L.smith, S.F.Chuang and S.D.Coliins, *J.Electron. Mater.* 17, 533, 1988.
14. A.Uhlir, *Bell System Tech. J.* 35, 333, 1956.
15. D.W.Cooke, R.E.Muenchausen, B.L.Bennett, L.G.Jacobsohn and M.Nastasi, *J.Appl. Phys.* 96, 197, 2004
16. L.Tsybeskov, Ju.V.Vandyshev and P.M.Fauchet, *Phys. Rev. B* 49, 7821, 1994.
17. A.J.Kontkiewicz, A.M.Kontkiewicz, J.Siejka, S.Sen, G.Nowak, A.M.Hoff, P.Sakthivel, K.Ahmed, P.Mukherjee, S.Witanachchi and J.Lagowski, *Appl. Phys. Lett.* 65, 1436, 1994.
18. H. Mizuno, H. Koyama and N. Koshida, *Appl. Phys. Lett.* 69, 3779, 1996.
19. M. V. Wolkin, J. Jorne, P. M. Fauchet, G. Allan and C. Delerue, *Phys. Rev. Lett.* 82, 197, 1999.
20. L. Luo, X. X. Zhang, K. F. Li, K. W. Cheah, J. X. Shi, W. K. Wong and M. L. Gong, *Adv. Mater.* 16, 1664, 2004.
21. K. Y. Suh, Y. S. Kim, S. Y. Park and H. H. Lee, *J. Electrochem. Soc.* 148, C439, 2001.
22. Y. S. Kim, K. Y. Suh, H. Yoon and H. H. Lee, *J. Electrochem. Soc.* 149, C50, 2002.
23. A.Givant, J.Shappir and A.Sa'ar, *Appl. Phys. Lett.* 73, 3150, 1998
24. G. Barillaro, A.Diligenti, F.Pieri, F.Fuso and M.Allegri, *Appl. Phys. Lett.* 78, 4154, 2001.
25. N.koshida, H.Koyoma, Y.Yamanoto and G.J.Collins, *Appl. Phys. Lett.* 63, 2655, 1993.
26. De Martini, Innocenti, G.R.Jacobovitz and P.Mataloni, *Phys. Rev. Lett.* 59, 2955, 1987.
27. H.Yokoyama, K.Nishi, T.Anan, H.Yamada, S.D.Broson, and E.P.Ippen, *Appl. Phys. Lett.* 57, 2814, 1992.
28. A.Trdicucci, Y.Chen, V.Pellegrini and C. Deparis, *Appl. Phys. Lett.* 66, 2388, 1995.
29. C.Weisbuch, M.Nishioka, A.Ishikawa and Y.Arakawa, *Phys. Rev. Lett.* 69, 3314, 1992.
30. H.A.MacLeod, *Thin-Film Optical filters*, Adam Hilger, London, 1969.
31. J.D.Joannopoulos, R.D.Meade and J.N.Winn, *Photonic Crystals: Molding the flow of Light*, Princeton University press, Princeton, NJ, 1995.
32. L.Pavesi, *La Revista del Nuevo Cimento* 20, 18, 1997
33. K.H.Li, D.C.diaz, Y.He, J.C.Campbell and C.Tsai, *Appl. Phys. Lett.* 64, 2655, 1993
34. P.Steine, F. Kozlowski and W.Lang, *Appl. Phys. Lett.* 62, 2700, 1993.
35. L.Pavesi, M.Ceschini, G.Mariotto, E.Zanghellini, O.Bisi, M.Anderle, L.Calliari and M.Fedrizzi, *J.Appl. Phys.* 75, 1118, 1994.
36. L.Pavesi, *Rev. Nuevo Cimento* 20, 1, 1997
37. M.G.Berger, C. Dieker, M.Thonissen, L.Vescan, H.Luth, H.Munder, W.Thieß, M.Wernke and P.Goose, *J.Phys.D: Appl. Phys.* 27, 1333, 1994
38. C.Mazzoleni, and L.Pavesi, *Appl. Phys. Lett.* 67, 2983, 1995.
39. M.Araki, H.Koyama and N.Koshida, *Jpn. J.Appl. Phys.* 35, 2B 1041, 1996.
40. M.G.Berger, M.Thonissen, R.Arens-Fischer, H.Munder, H.Luth, M.Amtzen, W.Theiss, *Thin Solid Films*, 255, 313, 1995.
41. L.Pavesi, C.Mazzoleni, A.Tredicucci and V. Pellegrini, *Appl. Phys. Lett.* 67, 3280, 1995.
42. V.Pellegrini, A.Tredicucci, c.Mazzoleni and L.Pavesi, *Phys. Rev. B* 52, R14 328, 1995.
43. A.Loni, L.T.Canham, M.G.Berger, R.A.fischer, H.Munder, H.Luth, H.F.Arrand and T.M.Benson, *Thin solid films* 276, 143, 1996
44. M.Araki, H.Koyama and N.Koshida, *Appl. Phys. Lett.* 68, 2999, 1996.
45. M.Kruger, M.Marso, MGBerger, M.Thonissen, S.Billat, R.Loo, W.Reets, H.Luth, S.Hilbrich, R.Arens-Fischer, P.Grosse, *Thin Solid Films.* 297, 241, 1997.
46. L.Pavesi, R.Guardini and C.Mazzoleni, *Sol. State Commun.* 97, 1051, 1996
47. M.Araki, H.Koyama and N.Koshida, *Appl. Phys. Lett.* 69, 2956, 1996
48. S.Chan and P.M.Fauchet, *Appl Phys. Lett.* 75, 274, 1999.
49. L.Pavesi and P.Dubos, *Semicon. Sci.Techno.* 12, 570, 1997.
50. P.J.Reece, G. Lerondel, w.H.Zheng and M.Gal, *Appl. Phys. Lett.* 81, 4895, 2002.
51. M.Ghulinyan, C.J.Oton, G.Bonetti, Z.Gaburro and L.Pavesi, *J.Appl. Phys.* 93, 9724, 2003.

52. M. B. H. Breese, E. J. Teo, D. Mangaiyarkarasi, F. Champeaux, A. A. Bettiol and D. J. Blackwood, *Nucl. Instrum. Methods Phys. Res. B* 23, 357, 2005.
53. D. Mangaiyarkarasi, E. J. Teo, M. B. H. Breese, A. A. Bettiol, & D. J. Blackwood, *J. Electrochem. Soc.* 152, D173, 2005.
54. E. J. Teo, M. B. H. Breese, A. A. Bettiol, D. Mangaiyarkarasi, F. J. T. Champeaux, F. Watt and D. J. Blackwood, *Adv. Mater.* 18, 51, 2005.
55. E. J. Teo, D. Mangaiyarkarasi, M. B. H. Breese, A. A. Bettiol, D. J. Blackwood, *Appl. Phys. Lett.* 85, 4370, 2004.
56. J.C. Maxwell-Garnett, *Philos. Trans. R. Soc. London* 203, 385, 1904.
57. D.A.G. Bruggemann, *Ann. Phys.* 24, 636, 1925.
58. H. Looyenga, *Physica* 31, 401, 1965.
59. G. Vincent, *Appl. Phys. Lett.* 64, 2367, 1994
60. L. Pavesi, *Microelectronics J.* 27, 437, 1996.